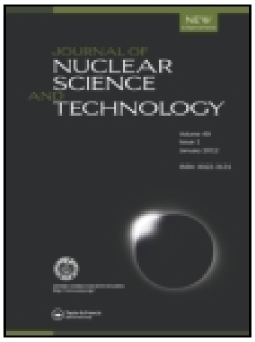

Journal of Nuclear Science and Technology

ISSN: 0022-3131 (Print) 1881-1248 (Online) Journal homepage: https://www.tandfonline.com/loi/tnst20

Monte Carlo Simulation of a CZT Detector

Sung Dae Chun, Se Hwan Park, Jang Ho Ha, Han Soo Kim, Yoon Ho Cho, Sang Mook Kang, Yong Kyun Kim & Duk Geun Hong

To cite this article: Sung Dae Chun, Se Hwan Park, Jang Ho Ha, Han Soo Kim, Yoon Ho Cho, Sang Mook Kang, Yong Kyun Kim & Duk Geun Hong (2008) Monte Carlo Simulation of a CZT Detector, Journal of Nuclear Science and Technology, 45:sup5, 549-552, DOI: 10.1080/00223131.2008.10875913

To link to this article: https://doi.org/10.1080/00223131.2008.10875913

Published online: 27 Aug 2014.

Journal of NUCLEAR SCIENCE and TECHNOLOGY, Supplement 5, p. 549–552 (June 2008)

Monte Carlo Simulation of a CZT Detector

Sung Dae CHUN[1,2], Se Hwan PARK[1], Jang Ho Ha[1], Han Soo KIM[1], Yoon Ho CHO[3], Sang Mook KANG[3], Yong Kyun KIM[3*], and Duk Geun HONG[2]

[1]*Korea Atomic Energy Research Institute, Dukjin-dong, Yuseong-gu, Daejeon, Korea*
[2]*Kangwon National University, Hyoja-dong, Chuncheon, Korea*
[3]*Hanyang University, Haengdang-dong, Seongdong-gu, Seoul, Korea*

CZT detector is one of the most promising radiation detectors for hard X-ray and γ-ray measurement. The energy spectrum of CZT detector has to be simulated to optimize the detector design. A CZT detector was fabricated with dimensions of 5×5×2 mm^3. A Peltier cooler with a size of 40×40 mm^2 was installed below the fabricated CZT detector to reduce the operation temperature of the detector. Energy spectra of were measured with 59.5 keV γ-ray from ^{241}Am. A Monte Carlo code was developed to simulate the CZT energy spectrum, which was measured with a planar-type CZT detector, and the result was compared with the measured one. The simulation was extended to the CZT detector with strip electrodes.

KEY WORDS: CZT detector, Monte-Carlo code, planar-type detector, strip electrode

I. Introduction

Cadmium Zinc Telluride (CZT) detector has been developed to obtain the high energy resolution spectrum at room temperature. It is employed in many application areas, which include medical imaging, industrial process monitoring, homeland security, environmental safety, and basic science. It was made possible with improvements in large volume crystal growth and surface treatment[1-2].

A CZT detector has high potential because of its wide band gap and high atomic number. The wide band gap enables a CZT detector to be used at room temperature without cooing system. A CZT detector is compact and easy to handle. However, tailing due to carrier trapping is still a major problem when CZT detector is used in X-ray or γ-ray spectrometry. Tailing is usually characterized by charge trappings of electrons and holes. Hence, mean free path of electrons and holes are necessary to calculate the response functions of the CZT detector[3].

In the previous works, the modeling of charge transport in CZT detector was studied. Hamel solved analytically the transport equation for charge carriers drifting in a linearly varying field[4]. Heanue first calculated the path of the change carrier and then solved numerically a one dimensional transport equation along this curve path[5]. Prettyman combined charge carrier drift and signal include computations in a two dimensional model to produce a two dimensional Charge Induction Efficiency map. It was used in a Monte Carlo calculation to the pulse height spectrum[6]. The model was developed to study the influence of material parameters; mobility, trapping, detrapping, electric field distribution. However, it was limited to the simulation of planar detectors[7]. Park developed a simulation code to calculate the energy response of the CZT detector[8]. The mean free paths of electron and hole were determined from the shape of the energy spectrum. At first, the mean free paths of the electron was extracted from the bias dependence of α-particle spectrum, and that of the hole was extracted from the comparison between the measured and the simulated γ-ray spectrum.

In this work, we measured with the γ-ray of 59.5 keV from ^{241}Am and the results were compared with simulation results. The obtained mean free paths were compared with the other group's calculated results. The simulation was extended to the energy spectrum of CZT strip detector.

II. Experiment

The CZT detector employed a spectroscopic grade crystal with the dimensions of 5×5×2 mm^3 and 5×5×5 mm^3. It was obtained from eV products and a division of II-VI incorporated. It was known that the Pt electrodes were deposited on both sides of the CZT detector. The signal electrode of 5×5×5 mm^3 dimensions was connected to a metal plate with a conductive epoxy. **Fig. 1** shows the experimental setup. A Peltier cooler with the size of 40 × 40 mm^2 was installed below the CZT detector. Water jacket was placed below the cooler to reduce the temperature. Thermocouple was placed close to the CZT detector to monitor the temperature of the CZT detector. **Fig. 2** shows experimental setup to measure the energy spectrum as the temperature of the CZT crystal was changed. The signal from the detector was passed through the charge-sensitive preamplifier (eV products Model 550), and the amplifier (ORTEC Model 572). The shaping time of amplifier was 1 μ sec. High voltage was biased on the detector with a high voltage power supply (ORTEC Model 659). The energy spectra were measured at the varying temperature. A pulse generator (ORTEC 480) was connected to the preamplifier to check the electronic noise.

*Corresponding Author, Tel. +82-2-2220-2354, Fax. +82-2-2296-2354, E-Mail; ykkim4@hanyang.ac.kr, ex-spark@kaeri.re.kr

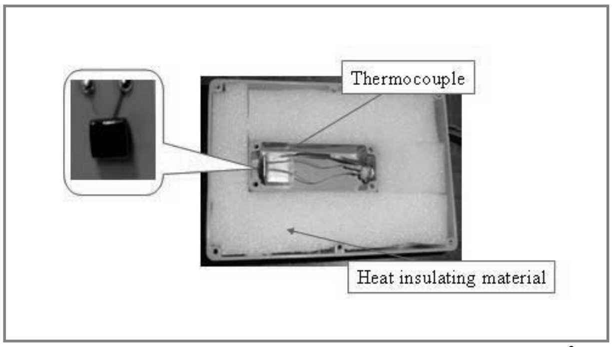

Fig. 1 The experimental setup dimensions of 5×5×2 mm[3] CZT detector

A commonly used method to study the transport properties in detectors is based on their response to α-particles. This method requires a specialized apparatus that allows the radiation source to be in close proximity to the detector, since α-particles will not penetrate more than a few microns through solid matter and will scatter inelastically even from air. Because the penetration depth of α-particles is only a few microns, the single-particle Hecht relation can be used to explain the measured circles[1)]:

$$Q(V) = \frac{qVN_0(\mu\tau)_e}{d^2}\left[1-\exp\left(\frac{d^2}{(\mu\tau)_e V}\right)\right] \quad (1)$$

where N_0 is the number of charge carriers created by the incident radiation, Q the total charge collected, d the distance between the cathode and the anode. q the electronic charge, and V is the bias voltage. By measuring the charge collection with a long shaping time as a function of bias and fitting the data to the equation, $(\mu\tau)_e$ is the mobility-trapping time products for electron. Data was fitted with Eq. 1. From the fitting result, we could determine $(\mu\tau)_e$ of the CZT detector to be 1.69×10^{-3} cm^2/V.

The γ-ray energy spectrum was measured with the CZT detector. ^{241}Am with an activity of 45.6 nCi. was placed 70 cm away from the detector. Since the distance between the radiation source and the detector was quite long, it could be expected that parallel beam would be incident on the detector. The energy spectra were measured with various bias voltages. In all of the measurements, the dead times were less than 3%. **Fig. 3** shows γ-ray energy spectra measured with the CZT detector. The spectra were measured the temperature from -1.1℃ to 40℃. The energy spectrum measured with the bias voltage of 400 V showed the best energy resolution. When the bias voltage was higher than 400 V, the energy resolution got worse, and it would be from the increase of the dark current of the CZT detector. The α-spectrum was measured with the CZT detector. ^{238}Pu with an activity of 76.5 nCi. was placed 1.0 mm away from the detector. **Fig. 4** shows α-spectrum measured with the CZT detector. The spectrum was measured the temperature -4.6 ℃. The energy spectrum measured with the bias voltage of 200 V.

When the electron had to travel longer distance, the energy spectrum showed clear full energy peak. The energy spectra with the clear full peak were only employed to determine the mean free paths of the charge carriers in CZT crystal.

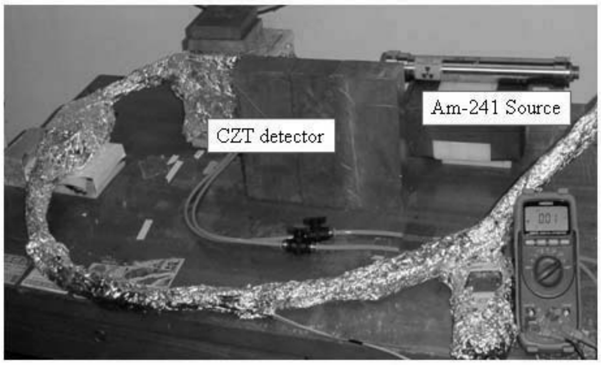

Fig. 2 Experimental setup to measure the energy spectrum as the temperature of the CZT crystal was changed

III. Simulation of the Response Function

The energy spectrum with the bias voltage of 500V was calculated with simulation, and it was fitted simultaneously to the measured ones. **Fig. 5** shows the results of the fitting.

The CZT material data was created with PEGS4 using a density of 5.86 g/cm^3. The energy limits in PEGS4[10)] were chosen to be AP=0.001, UP=10.0, AE=0.512, and UE=10.0 MeV for photons and electrons, respectively. Electron-hole pairs were created whenever energy was deposited in a semiconductor. The average energy required to create an electron-hole pair was denoted as the W value, which was used 4.6 eV for CZT. The output pulse was proportional to the collected charge which was controlled primarily by mobility-lifetime products, $(\mu\tau)_e$ and $(\mu\tau)_h$ (units: cm^2/V), for electrons and holes, respectively. The mobility of charge carriers in CZT were much smaller than in Si and Ge detectors and the charge carriers were easily trapped in the crystal while they moved to the electrodes.

The charge collection efficiency was defined as the ratio of the number of charge carriers collected at the electrodes to the total number of carriers generated by radiation energy deposition. If the effect of de-trapping was neglected, the charge collection efficiency η(z) for charge carriers at depth z in a semiconductor crystal of thickness d (cm) could be expressed with Hecht equation[8)].

$$\eta(z) = \frac{V(\mu\tau)_e}{d^2}\left[1-\exp\left(\frac{d^2}{(\mu\tau)_e V}\right)\right] + \frac{V(\mu\tau)_h}{d^2}\left[1-\exp\left(\frac{d^2}{(\mu\tau)_h V}\right)\right] \quad (2)$$

where both electrons and holes contributions were included, respectively. Here z is the depth into the crystal from the negatively-biased front surface.

The symmetrical peak broadening was from the electronic noise, statistics of the charge carriers, and the leakage current. The symmetrical peak broadening was approximated with the Gaussian shape. The peak broadening due to the electronic noise and the leakage current was estimated from the pulse spectrum. The peak broadening due to the statistics of the charge carriers was included with:

$$\Gamma_{stat} = 2.35\sqrt{FWE} \qquad (3)$$

where Γ_{stat} is the FWHM due to the statistics of the charge carrier, F is the Fano factor, having a value between 0.1 and 0.2 for CdZnTe[15], W the mean energy necessary to create one electron-hole pair, and E was the incident energy.

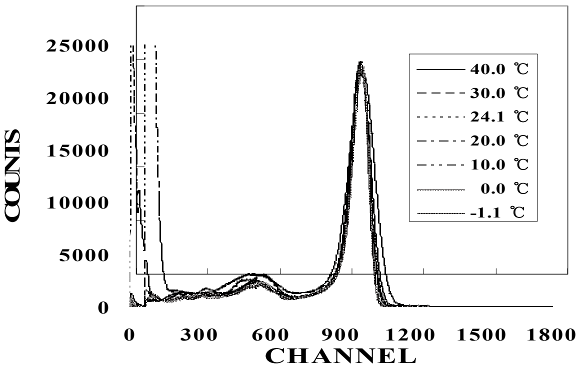

Fig. 3 γ−ray energy spectra measured with the CZT detector. The spectra were measured temperature from -1.1℃ to 40℃.

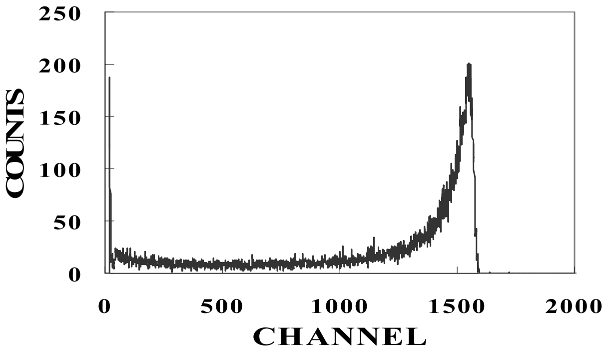

Fig. 4 α−spectrum measured with the CZT detector. The spectrum was measured temperature -4.6℃.

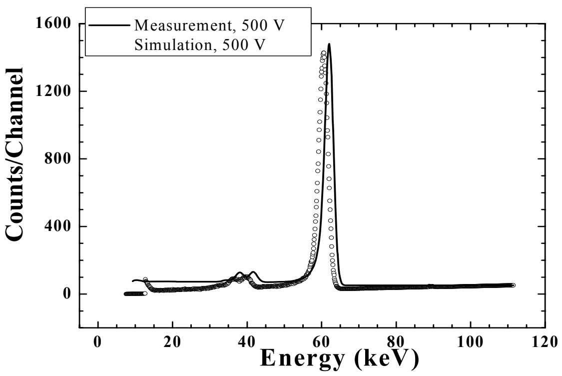

Fig. 5 The measured and the simulated energy spectra of 59.5 keV γ−ray.

From the fitting, $(\mu\tau)_h$ was determined to be 3.76×10^{-5} cm^2/V. The data obtained in our previous work was consistent with previously known values. A measure of the variations found in measured mobility is shown in Table 1., where $(\mu\tau)_e$ and $(\mu\tau)_h$ values from a number of others are presented.

The simulation was extended to the energy spectrum measured with strip-electrode CZT detector. When the CZT detector with strip electrode was used to measure the energy spectrum, more elaborate method had to be included. That is, weighting potential should be used to obtain the induced signal on the electrode. The incoming radiation generated moving charge within the detector, and charge was induced on the electrode by the movement of charge in the detector. The induced charge was amplified and shaped to the output signal. Because unique relation was established between the incoming radiation and the induced signal on the electrode, the radiation could be measured with the detector. The time dependence of the induced charge could be calculated as function of instantaneous position of moving charge in the detector. However, these processes were too tedious to be used in the real calculation. Schockley-Ramo theorem gave quite simple method to obtain the induced charge on the electrode by introducing weighting potential.

Table 1 Selected transport properties of CZT in published papers

Author	Year	$(\mu\tau)_e$ (cm^2/V)	$(\mu\tau)_h$ (cm^2/V)
Olschner[9]	1989	2.0×10^{-3}	7.0×10^{-5}
Hamilton[11]	1994	3.0×10^{-3}	
Heanue[12]	1996	2.3×10^{-3}	1.8×10^{-5}
Z. He[13]	2000	5.4×10^{-3}	
J.C. Liu[10]	2000	7.0×10^{-3}	5.0×10^{-5}
Schlesinger[1]	2001	3.30×10^{-3}	
S. Miyajima[3]	2002	1.0×10^{-1}	2.0×10^{-5}
S. H. Park[8]	2007	1.69×10^{-3}	3.76×10^{-5}

The weighting potential was calculated with the analytical expression, which was proposed by He[14]. The obtained weighting potential is shown in **Fig. 6.**

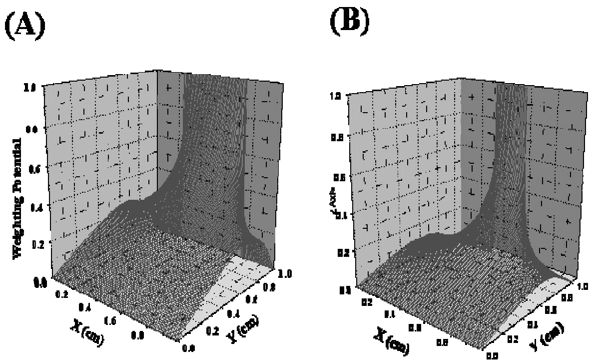

Fig. 6 Calculated weighting potentials. The right one (B) was calculated when the electrode width was 5 mm, and the left one (A) was calculated when the electrode width was 2.5 mm. As the

electrode width got thinner, the potential became steeper.

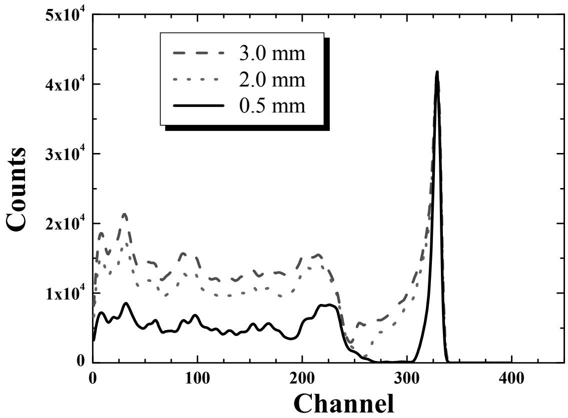

Fig. 7 The calculated energy spectra of detector with strip electrode. The size of the detector was 10×10×10 mm^3.

The number of charge carriers and the generation positions of charge carriers in the detector were calculated with EGSnrc[10)]. The induced charge was obtained from the calculated weighting potential. The simulated energy spectra were shown in **Fig. 7**.

As one could see, the tail in lower energy region could be reduced when the strip electrode width got thinner. The comparison between the measurement and the simulation is underway.

IV. Conclusion

The energy resolution was improved from 12.5 % to 8.4 % when the detector temperature was changed from 40.0 ℃ to -1.1 ℃. The spectrum distortion can be characterized by the mean free path of the charge carriers. It was obtained from the measurement of the α-spectrum and γ-spectrum. A Monte Carlo simulation was developed and the result was compared with the experimental one. The simulation was extended to the case, where the energy spectrum was measured with the strip electrode. Our work could be helpful to design the CZT detector for high-resolution energy spectroscopy.

Acknowledgments

This work has been carried out under the nuclear R&D program of the Ministry of Science and Technology (MOST) of Korea. We are also supported by the iTRS Science Research Center / Engineering Research Center program of MOST / Korea Science and Engineering Foundation.

References

1) T.E. Schlesinger, J.E. Tonet, H. Yoon, E.Y. Lee, B.A. Brunett, L. Franks, and R.B. James, Materials Science and Engineering, 32 (2001) 103.
2) R. González, J.M. Perez, Z. He, Nucl. Instr. Meth. A 541 (2004) 554.
3) S. Miyajima, H. Sakuragi, M. Matsumoto, Nucl. Instr. and Meth. A 485 (2002) 533.
4) L.A. Hamel, S. Paquet, Nucl. Instr. and Meth. A 380 (1996) 238.
5) J.A. Haenue, J.K. Brown, B.H. Hasegawa, IEEE Transactions on Nuclear Science, NS-44 (3) (1997) 701.
6) T.H. Prettyman, Nucl. Instr. and Meth. A 422 (1999) 232.
7) A. Glière, M. Rosaz, L. Verger, Nucl. Instr. and Meth. A 442 (1999) 250.
8) S.H. Park, Y.K. Kim, S.D. Jeon, J.H. Ha, D.G. Hong, Nucl. Instr. Meth. A In press (2007).
9) Olschner, J.C. Lund, and I. Stern, IEEE Transactions on Nuclear Science, 36 (1989) 1176.
10) J.C. Liu, W.R. Nelson and R. Seefred, KEK proceedings 200-20 (2000) 135.
11) W.J. Hamilton, D.R. Ringer, S. Sen, M.H. Kalisher, K.James, C.P. Reid, V. Gerrish, C.O. Baccash, IEEE NS-41 (4) (1994) 989.
12) J.A. Haenue, J.K. Brown, B.H. Hasegawa, Nucl. Instr. and Meth. A 380 (1996) 392.
13) Z. He, W. Li, G.F. Knoll, D.K. Wehe, C.M. Stahle, Nucl. Instr. and Meth. A 441 (2000) 459.
14) Z. He, Nucl. Instr. Meth. A 365 (1995) 572.
15) B.P.F. Driks, C. Daly. O. Gevin, O. Limousin, F. Lugiez, Nucl. Instr. and Meth. A 567 (2006) 145.